Planet. Space Sci., Vol. 26, pp. 339 to 345. Pergamon Press, 1978. Printed in Northern Ireland

MAGNETIC ORDERING OF THE POLAR AIRGLOW

J. E. FREDERICK and P. B. HAYS
Space Physics Research Laboratory, Department of Atmospheric and Oceanic Science, The University of Michigan, Ann Arbor, MI 48109 U.S.A.

(*Received* 19 *September* 1977)

Abstract—The visible airglow experiment on the Atmosphere Explorer-C satellite has gathered sufficient data over the Earth's polar regions to allow one to map the geographic distribution of particle precipitation using emissions at 3371 and 5200 Å. Both of these features exhibit large variations in space and time. The 3371 Å emission of $N_2(C^3\pi)$, excited by low energy electrons, indicates substantial energy inputs on the dayside in the vicinity of the polar cusp. More precipitation occurs in the morning than evening for the sample reported here, while the entire night sector between magnetic latitudes 65° and 77.5° is subjected to particle fluxes. Regions of enhanced 5200 Å emission from $N(^2D)$ are larger in horizontal extent than those at 3371 Å. This smearing effect is due to ionospheric motions induced by magnetospheric convection.

INTRODUCTION

The composition and temperature structure of the high latitude thermosphere is largely controlled by particle precipitation and joule heating. Motion systems initiated by these energy inputs lead to the well-known N_2 enhancements which exist over the poles in both disturbed and quiet magnetic conditions (Hedin and Reber, 1972; Hays *et al.*, 1973a, Taeusch and Hinton, 1975), however, measurements of bulk composition do not allow one to view the separate effects of particle and electrodynamic heating. Selected airglow emissions can be responsive to particles only or to both of the above processes and thus provide remote sensors of the two high latitude energy sources. We here discuss the distribution of the $N_2(C^3\pi)$, 3371 Å, and $N(^2D)$, 5200 Å, emissions over the polar regions as monitored by the visible airglow experiment (VAE) on the Atmosphere Explorer-C (AE-C) satellite. The former emission responds to particle precipitation alone while the latter is an index of both particle and electrodynamic energy inputs.

AIRGLOW EXCITATION MECHANISMS

Excitation of the $C^3\pi$ state of N_2 is spin forbidden from the ground state so the solar photon flux provides a negligible source of the excited molecule. The only excitation is by energetic electron impact on N_2:

$$e^* + N_2 \rightarrow N_2(C^3\pi) + e, \quad (1)$$

followed by a downward transition giving the second positive bands:

$$N_2(C^3\pi) \rightarrow N_2(B^3\pi) + h\nu. \quad (2)$$

The radiative transition is fully allowed so that quenching is unimportant. The (0–0) band provides the 3371 Å emission and is excited by electrons in the energy range 11.1 eV to roughly 40 eV. Kopp *et al.* (1977) give further details of the transition as observed in the mid-latitude dayglow. At high latitudes the 3371 Å feature is excited by degraded primary electrons or, more important, the secondary electron spectrum. The emission is therefore a good indicator of the spatial extent of a precipitation region.

Excitation of the metastable ^2D term of atomic nitrogen is accomplished by several processes. The major source at mid-latitudes below 280 km is dissociative recombination of NO^+:

$$NO^+ + e \rightarrow N(^2D) + O, \quad (3)$$

followed in importance by:

$$N_2^+ + O \rightarrow NO^+ + N(^2D), \quad (4)$$

and:

$$e^* + N_2 \rightarrow N + N(^2D) + e. \quad (5)$$

The contribution of

$$N_2^+ + e \rightarrow N + N(^2D) \quad (6)$$

is comparable to reaction 5 between 220 and 240 km and increases rapidly in importance at higher altitudes. For further details on the 5200 Å mid-latitude dayglow, see Frederick and Rusch (1977). The major losses of $N(^2D)$ are quenching by atomic oxygen and electrons and reaction with O_2. The actual 5200 Å emission accounts for a negligible loss due to the highly metastable nature of the excited state. The production of $N(^2D)$ requires a

somewhat larger energy than that of $N_2(C^3\pi)$, but the 5200 Å emission nonetheless provides a map of particle inputs. However, as described below, thermospheric motions also influence the spatial pattern of the 5200 Å surface brightness.

Reaction 4 is the major source of NO^+ is daylight while at altitudes of interest here

$$O^+ + N_2 \rightarrow NO^+ + N(^4S), \qquad (7)$$

provides roughly 30% of the total. The production of $N(^2D)$ in reaction 7 is not energetically allowed. The lifetime of O^+ is sufficiently long that its distribution over the polar region is controlled by the ion drift velocity. The reader is referred to Heelis *et al.* (1976) and references therein for discussions of motions in the polar thermosphere induced by magnetospheric convection. A rate coefficient of 6×10^{-13} cm^3 s^{-1} for reaction 7 (Lindinger *et al.*, 1974) and typical high latitude N_2 number densities give an O^+ lifetime of $\tau(O^+)\approx1.2-2.3\times10^3$ s at 240 km and $\tau(O^+)\approx5.0-9.7\times10^3$ s at 280 km. The factor of two spread at each altitude allows for possible temporal variations in N_2 at high latitudes with the smaller $\tau(O^+)$ values corresponding to disturbed magnetic conditions. Oxygen ions produced by particle precipitation or transported into the polar cusp from lower latitude daylight regions provide a source of $N(^2D)$ through reactions 7 and 3. If we adopt a typical O^+ lifetime of one hour and a convective velocity of 1 km s^{-1}, then metastable nitrogen atoms can spread over the entire polar cap. The assumed convection velocity is typical of the higher values measured on AE-C which tend to occur short distances on either side of the boundary between open and closed field lines (Heelis *et al.*, 1976). The chemical lifetimes of NO^+ and N_2^+ are too short for these ions to be influenced by transport. However, ion convection velocities near 1 km s^{-1}, when communicated to the neutrals, influence the spacial extent of $N(^2D)$ prior to its chemical destruction. The characteristic time for chemical removal of $N(^2D)$ is:

$$\tau_c = \frac{1}{k(O)[O]+k(O_2)[O_2]+k(e)[e]}$$

where $k(i)$ is the rate coefficient for $N(^2D)$ loss by collision with constituent i. Use of the rate coefficients of Frederick and Rusch (1977) and typical species concentrations measured onboard AE-C (Mauersberger *et al.*, 1976; Brace *et al.*, 1973; Frederick and Rusch, 1977) give:

$$\tau_c \approx 8.5\times10^2 \text{ s at } 240 \text{ km}$$

$$\tau_c \approx 1.3\times10^3 \text{ s at } 280 \text{ km}.$$

The characteristic transport time is:

$$\tau_t = L/v_c,$$

where $v_c \approx 1$ km s^{-1} is the convection velocity and L is a length scale taken as 5–10 degrees of latitude. Hence,

$$\tau_t \approx 5.5\times10^2 - 1.1\times10^3 \text{ s}.$$

Chemistry and convective transport are competitive at F-region heights. Near regions of particle precipitation the direct production and transport of $N(^2D)$ will dominate in determining the distribution. In areas removed from a particle flux by more than 5–10 degrees of global circumference transport of O^+ will supply the $N(^2D)$ source. Observation of the 5200 Å emission over the polar cap thereby provides a monitor of thermospheric response to magnetospheric convection. As discussed below, the orbit of AE-C allows only a limited study of this effect.

DATA ACQUISITION AND ANALYSIS

The orbit of the AE-C satellite is inclined at 68° to the equator and hence, the region above a magnetic latitude (Λ) of 70° is viewed only when the magnetic coordinates are favorably situated with respect to the geographic. Polar areas above $\Lambda = 80°$ are seldom reached and do not receive attention here. We concentrate on the region between $\Lambda = 65$ and 80° which includes the nightside auroral zone and the dayside polar cusp. Late in the mission AE-C was placed in a near-circular orbit at altitudes in the range 230–255 km. The present study is based on data from this time period.

Hays *et al.* (1973b) have described the VAE instrument on AE-C. We here use surface brightness values obtained by the wide angle photometer (3° half-angle cone) looking in the vertical direction. A filter wheel steps through six positions and we have selected the 3371 and 5200 Å measurements from this set. The data reported here were taken during a two month period from mid-February to mid-April 1975. For this interval 30 orbits containing both 3371 and 5200 Å emissions were available which passed over the proper geographic regions. Because of the limited information base surface brightnesses from both the northern and southern hemispheres were combined.

The measured signal is contaminated by both a galactic emission and a solar u.v.-excited airglow. The galactic background at each wavelength was determined from five orbits flown during the elliptical phase of the AE-C mission at altitudes above

500 km. The adopted values are 14 and 3.4R at 5200 and 3371 Å respectively. Removal of the photon-excited airglow introduces a major uncertainty. However, the aim of this analysis is to examine the spatial extent of precipitation regions and to isolate effects of ionospheric motions on the resulting emissions. High accuracy in the absolute surface brightnesses is not required. The background airglow is primarily a function of solar zenith angle which varies on a given orbit as AE-C passes over the polar region. We approximate this by:

$$4\pi I(\text{u.v.}) = Ae^{-B\theta},$$

where $4\pi I$(u.v.) is the photon-excited contribution to the signal and θ is the solar zenith angle. The constants A and B are determined by plotting the measured surface brightnesses, with galactic background removed, as a function of θ at sub-auroral latitudes ($\Lambda = 55$–$60°$) and fitting the exponential form to the data. Figure 1 is the resulting plot for the 5200 Å emission. This statistical background was used in constructing maps of the particle-induced airglow. When comparing 3371 and 5200 Å measurements on a specific orbit it was sometimes possible to determine a more accurate background from data taken before and after the polar crossing. In many cases, however, a given orbit had data only before or only after the polar pass, necessitating a statistical approach to the background subtraction when combining surface brightnesses from many orbits. Figure 2 gives the measured overhead surface brightnesses on orbit 6269, and Fig. 3 presents the same measurements with all backgrounds removed. The solar zenith angle varied between 63 and 70° so that the corrections are quite large. Due to the uncertainties involved, any structure in the corrected surface brightnesses below the 10 Rayleigh level is not considered significant. Note in Fig. 3 the extent to which the background removal accents particle-induced emission peaks.

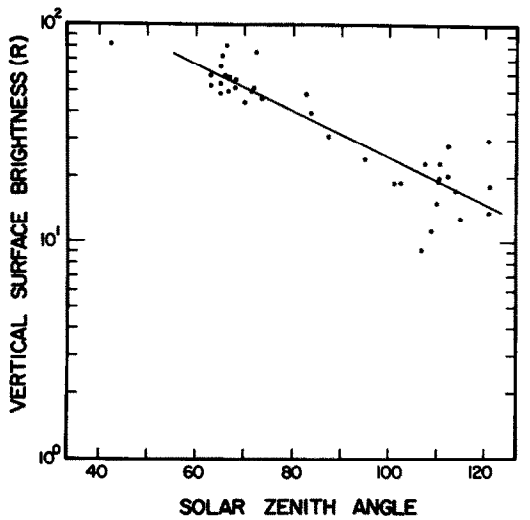

FIG. 1. OVERHEAD SURFACE BRIGHTNESS AT 5200 Å AS A FUNCTION OF SOLAR ZENITH ANGLE FOR MAGNETIC LATITUDES BETWEEN 55° AND 60°. GALACTIC BACKGROUND HAS BEEN REMOVED. THE SOLID LINE IS AN EXPONENTIAL FIT TAKEN AS THE PHOTON-EXCITED AIRGLOW BACKGROUND AT HIGHER LATITUDES.

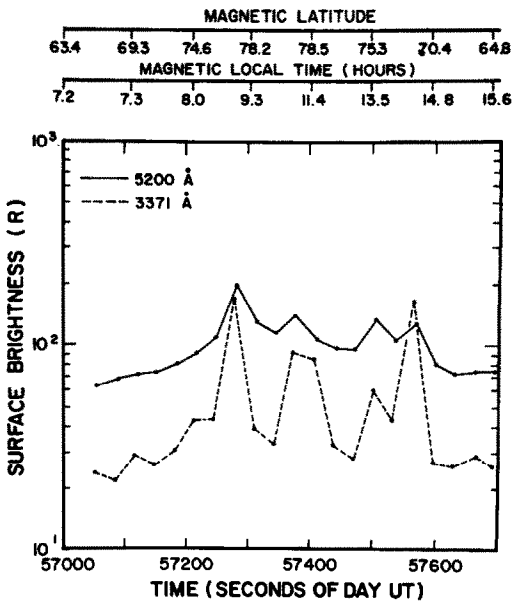

FIG. 2. MEASURED OVERHEAD 5200 AND 3371 Å SURFACE BRIGHTNESSES ON AE-C ORBIT 6269. THE PLOTTED EMISSIONS INCLUDE THE GALACTIC AND PHOTON-EXCITED BACKGROUNDS. THE ABSCISSA IS UNIVERSAL TIME IN SECONDS OF THE DAY.

RESULTS

Figures 3–5 present the 3371 and 5200 Å particle-induced emissions on orbits 6269, 6222 and 6496 respectively. Each point on the plot represents the signal measured in one 128 ms integration period. The individual orbital paths are shown in Fig. 6 as functions of magnetic latitude and magnetic local time. In all cases the 3371 Å feature shows a high degree of spatial structure indicating the presence of discrete particle streams. The largest surface brightnesses appear in the region $\Lambda = 75$–$80°$ between local times of 0900 h and noon. Orbits 6269 and 6222 show an additional

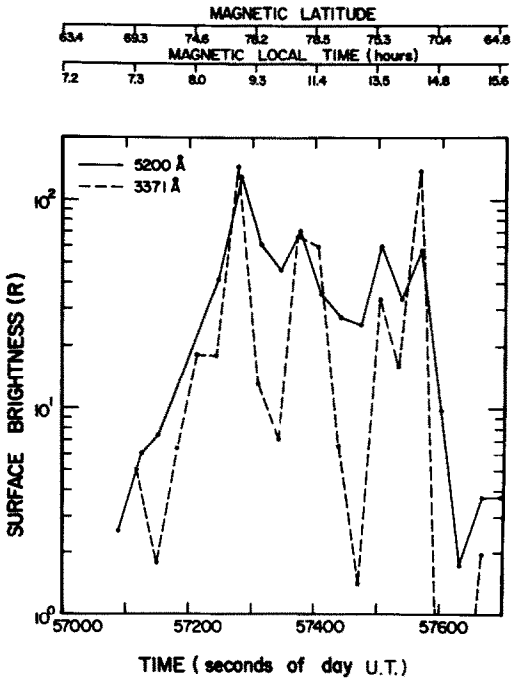

FIG. 3. OVERHEAD SURFACE BRIGHTNESSES ON ORBIT 6269 AFTER REMOVAL OF THE GALACTIC AND PHOTON-EXCITED CONTRIBUTIONS.

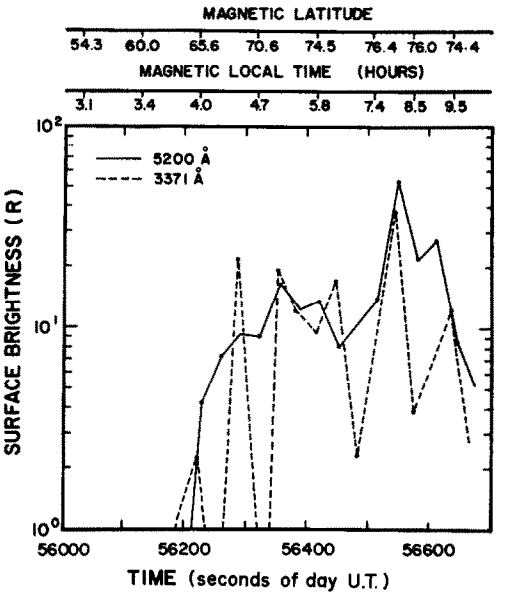

FIG. 5. OVERHEAD SURFACE BRIGHTNESSES AT 5200 AND 3371 Å ON AE-C ORBIT 6496. ALL BACKGROUNDS HAVE BEEN REMOVED.

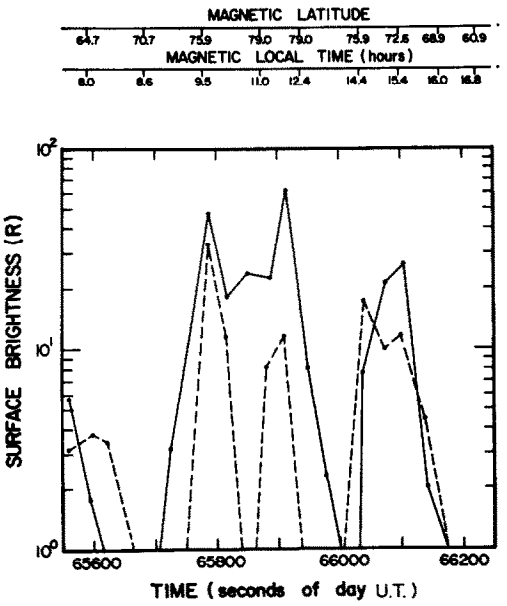

FIG. 4. OVERHEAD SURFACE BRIGHTNESSES AT 5200 AND 3371 Å FOR AE-C ORBIT 6222. ALL BACKGROUNDS HAVE BEEN REMOVED.

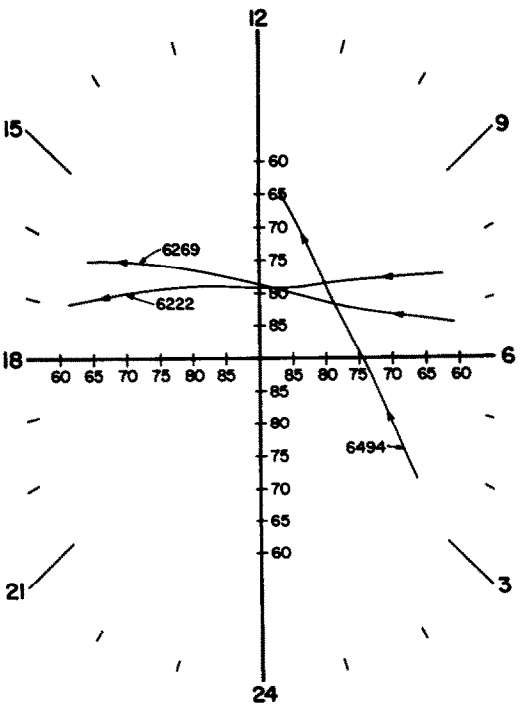

FIG. 6. PATHS OF ORBITS 6222, 6269 AND 6496 ACROSS THE NORTH POLAR REGIONS. COORDINATES ARE MAGNETIC LATITUDE AND MAGNETIC LOCAL TIME.

3371 Å enhancement near 1350–1500 hours in the $\Lambda = 70$–$75°$ band. Segments of the orbits between noon and 1350 hours show no significant emission. The data of Fig. 5 refer to the morning sector (magnetic local time = 3–9 hours) and extend to lower magnetic latitudes than the previous orbits. The onset of localized particle streams occurs near $\Lambda = 65°$. Emissions near $\Lambda = 76°$ are much brighter than any seen at lower latitudes in the morning.

Comparison of the 3371 and 5200 Å surface brightnesses shows that peaks occur in approximately the same locations. Coincident maxima are not possible since the observations are not exactly simultaneous. Whereas the 3371 Å feature shows a spiked structure, the 5200 Å emission consists of maxima imposed on a generally bright background. We attribute this smearing effect to thermospheric motions induced by the convection electric field. Flow of the metastable nitrogen atoms tends to eliminate horizontal gradients generated by the discrete particle streams prior to the 5200 Å photon emission.

Figures 7 and 8 are polar maps giving average surface brightnesses at 3371 and 5200 Å respectively sorted into bins which measure 2.5° in magnetic latitude by 6 hours in magnetic local time. Each orbit was given equal weight in the averaging process regardless of the number of integration periods which fell in a specific bin. The most prominent feature in the 3371 Å map is the bright polar cusp region between $\Lambda = 72.5$ and 80° in the noon sector (0900–1500 hours) with the maximum occurring in the $\Lambda = 75$–$77.5°$ bin. The auroral zone appears between $\Lambda = 65$ and 70° in the midnight sector (2100–0300 hours), with weaker emissions between $\Lambda = 70$ and 75°. No significant emission ($4\pi I < 10R$) exists poleward of 77.5°. Significant surface brightnesses exist in the morning (0300–0900 hours) up to $\Lambda = 77.5°$ whereas no emission appears in the evening sector (1500–2100 hours).

The overall features of the 5200 Å distribution in Fig. 8 are similar to those at 3371 Å. The noon sector cusp is the brightest feature with considerable emission from adjacent magnetic latitude bins. Midnight sector emissions appear, however, they differ in detail from the 3371 Å features. Between $\Lambda = 65°$ and 70° the average 3371 Å surface brightness is greater than that at 5200 Å while the reverse is true between $\Lambda = 70°$ and 75°. This implies

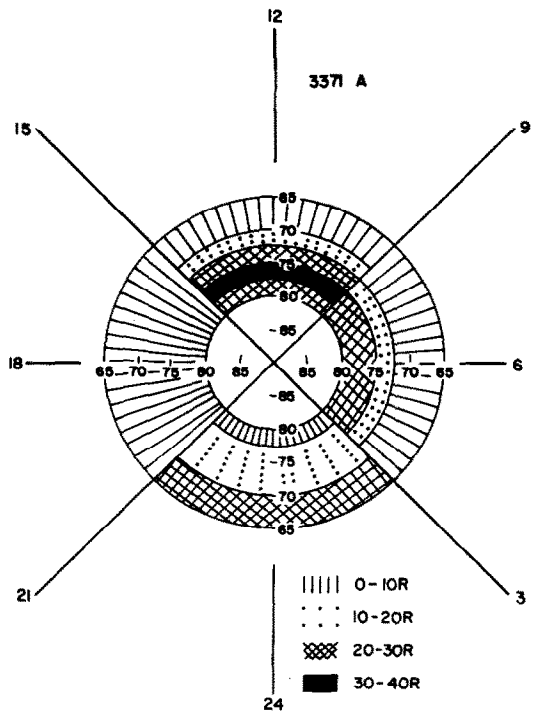

FIG. 7. POLAR MAP OF THE 3371 Å EMISSION. AVERAGE OVERHEAD SURFACE BRIGHTNESSES ARE GIVEN IN BINS MEASURING 2.5° IN MAGNETIC LATITUDE BY 6 HOURS IN MAGNETIC LOCAL TIME.

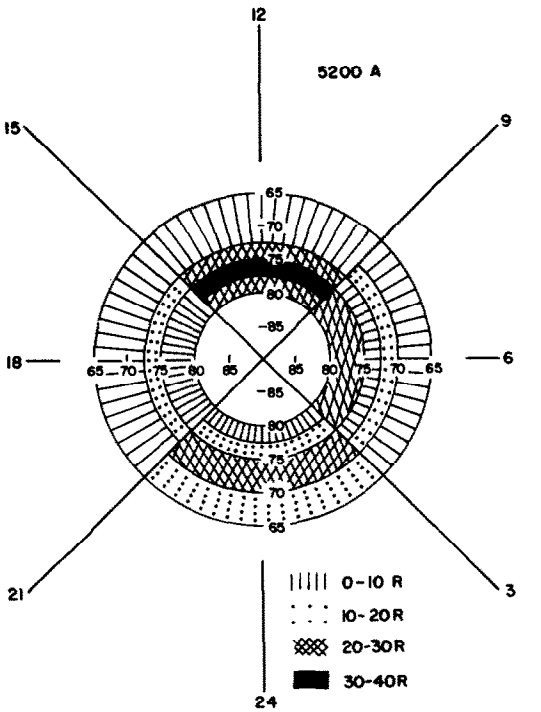

FIG. 8. POLAR MAP OF THE 5200 Å OVERHEAD SURFACE BRIGHTNESS AS A FUNCTION OF MAGNETIC LATITUDE AND MAGNETIC LOCAL TIME.

a nightside precipitation which becomes harder with increasing magnetic latitude until $\Lambda \sim 75°$ and then softens. The softening near $\Lambda = 75°$ is in agreement with direct particle measurements (Burch, 1971), however, the harder flux between $\Lambda = 70°$ and 75° as compared to $\Lambda = 65$–70° is not in accord with past auroral measurements (Eather, 1969; Eather and Mende, 1971). Caution is advised in comparing the AE-C data to ground or aircraft auroral measurements since only a small fraction of the incident energy flux is deposited above the satellite altitude.

More 5200 Å emission appears in the morning than in the evening, however, comparison of Fig. 7 and 8 reveals several differences. A band of weak 5200 Å signal appears in the evening sector between $\Lambda = 72.5$ and 75° and also in the morning at $\Lambda = 70$–72.5°. The 3371 Å surface brightness is below the significant level in these regions. It is possible that the enhanced 5200 Å signal represents a poor background subtraction. We note, however, that the bright bands nearly coincide with the expected boundary between open and closed field lines. Heelis *et al.* (1976) have reported large ion drift velocities on either side of this line so that a convective enhancement of the 5200 Å signal cannot be ruled out. The absence of significant 5200 Å emission between $\Lambda = 65°$ and 70–72.5° in all but the midnight sector implies that $N(^2D)$ enhancements associated with O^+ transport are small enough to be lost in the background subtraction when long term average surface brightnesses are studied.

Comparison of plots for individual orbits with the polar maps shows that the peak emissions observed on single passes are much larger than the average values for the entire 30 orbit set. A large variability exists in each bin. On the average each bin contains data from 9 to 11 separate orbits. Less data were available between $\Lambda = 77.5°$ and 80°. In all bins, one or more orbits existed which had no emission above background levels. Bright emissions appear most consistently in the noon sector between $\Lambda =$ 75° and 80°, but even here, 15–20% of the orbits showed insignificant signals. The $\Lambda = 77.5$–80° bin between 0300 and 0900 hours is an extreme case. Of 5 orbits with 5200 Å data only one, orbit 6269, had a large emission. As shown in Fig. 2 this emission is large enough to provide a significant average value for the bin. Note also that this signal was measured near the boundary between the noon and morning sectors. Hence, orbit 6269 probably represents an unusually intense excursion of noon-type particle precipitation into the morning sector. We have attempted to relate the emission magnitudes to the level of geomagnetic disturbance. The largest emission measured in a given bin occurred on a disturbed day in 50 per cent of the cases. See Lincoln (1975 a, b, c) for designations of disturbed and quiet days. However, 20% of the peak emissions occurred during quiet periods. Although a relationship between the polar airglow and geomagnetic indices probably exists, the present data base does not allow exploring it in detail. The large variability requires the polar maps to be interpreted as qualitative indicators of the time-averaged precipitation patterns. Individual orbits may differ drastically from the mean picture.

DISCUSSION

The emissions monitored by VAE imply a polar distribution of particle precipitation which is basically in accord with past airglow and flux measurements. An exception is the absence of emission in the evening sector. Eather and Mende (1971) observed similar features during both morning and evening, although their study contained no data in the approximate periods 1500–1800 and 0600–0900 hours. The 1500–2100 hours magnetic local time region in the present study contained less data than the other three quadrants, however, sufficient orbits were available to provide a meaningful picture. We conclude that precipitation in the morning quadrant is not necessarily similar to that in the evening as might be inferred from the conditions which prevailed during the measurements of Eather and Mende (1971). In general, a large variability is evident at all magnetic latitudes and local times.

The incoming particle flux does not consist of a uniform "drizzle" but rather precipitates in localized regions producing spikes in the 3371 Å distribution. The largest emissions occur in the vicinity of the dayside polar cusp. Enhancements in other airglow features have been observed in the same geographic region (Shepherd and Thirkettle, 1973). The influence of ionospheric motions in response to the convection electric field are readily visible in the 5200 Å distribution. Future quantitative analyses of the smearing effect may allow the atomic nitrogen emission to be used as a remote monitor of electrodynamic energy inputs to the polar thermosphere.

Acknowledgments—The authors thank Barbara K. Eby for her computing assistance. This work was supported by the National Aeronautics and Space Administration under Contract NAS5-23006 to the University of Michigan.

REFERENCES

Brace, L. H., Theis, R. G. and Dalgarno, A. (1973). The cylindrical electrostatic probes for Atmosphere Explorer-C, -D, and -E. *Radio Sci.* **8,** 341.

Burch, J. L. (1971). Low energy electron fluxes at latitudes above the auroral zone. *J. geophys. Res.* **73,** 3585.

Eather, R. H. (1969). Latitudinal distribution of auroral and airglow emissions, the "soft" auroral zone. *J. geophys. Res.* **74,** 153.

Eather, R. H. and Mende, S. B. (1971). Airborne observations of auroral precipitation patterns. *J. geophys. Res.* **76,** 1746.

Frederick, J. E. and Rusch, D. W. (1977). On the chemistry of metastable atomic nitrogen in the F-region deduced from simultaneous satellite measurements of the 5200 Å airglow and atmospheric composition, *J. geophys. Res.* **82,** 3509.

Hays, P. B., Jones, R. A. and Rees, M. H. (1973a). Auroral heating and composition of the neutral atmosphere. *Planet. Space Sci.* **21,** 559.

Hays, P. B., Carignan, G. R., Kennedy, B. C., Shepherd, G. G. and Walker, J. C. G. (1973b). The visible airglow experiment on Atmosphere Explorer. *Radio Sci.* **8,** 369.

Hedin, A. E. and Reber, C. A. (1972). Longitudinal variations of thermospheric composition indicating magnetic control of polar heat input. *J. geophys. Res.* **77,** 2871.

Heelis, R. A., Hanson, W. B. and Burch, J. L. (1976). Ion convection velocity reversals in the dayside cleft. *J. geophys. Res.* **81,** 3803.

Kopp, J. P., Rusch, D. W., Roble, R. G., Victor, G. A. and Hays, P. B. (1977). Photoemission in the second positive system of molecular nitrogen in the earth's dayglow. *J. geophys. Res.* **82,** 555.

Lindinger, W., Fehsenfeld, F. C., Schmeltekopf, A. L., and Ferguson, E. E. (1974). Temperature dependence of some ionospheric ion-neutral reactions from 300°–900°K, *J. geophys. Res.*, **79,** 4753.

Lincoln, J. V. (1975a). Geomagnetic and solar data. *J. geophys. Res.* **80,** 2340.

Lincoln, J. V. (1975b). Geomagnetic and solar data. *J. geophys. Res.* **80,** 2892.

Lincoln, J. V. (1975c). Geomagnetic and solar data. *J. geophys. Res.* **80,** 3284.

Mauersberger, K., Kayser, C., Potter, W. E. and Nier, A. O. (1976). Seasonal variation of neutral thermospheric constituents in the northern hemisphere. *J. geophys. Res.* **81,** 7.

Shepherd, G. G. and Thirkettle, F. W. (1973). Magnetospheric dayside cusp: A topside view of its 6300-Angstrom atomic oxygen emission. *Science* **180,** 737.

Taeusch, D. R. and Hinton, B. B. (1975). Structure of electrodynamic and particle heating in the undisturbed polar thermosphere. *J. geophys. Res.* **80,** 4346.